Characterization of the Nanostructures of a Lithographically Patterned Dot Array by X-ray Diffraction

D.R. Lee,[1] Y.S. Chu,[1] Y. Choi,[1] J.C. Lang,[1] G. Srajer,[1] V. Metlushko[2]
[1]Advanced Photon Source, Argonne National Laboratory, Argonne, IL, U.S.A.
[2]Department of Electrical and Computer Engineering, University of Illinois at Chicago, IL, U.S.A.

Introduction

Periodic arrays of nanostructured dots have attracted much attention during the last decade because of their potential as future high-density optical and magnetic storage media. The unique properties of these nanosystems depend strongly on their structural parameters, such as size, shape, and array spacing. X-ray scattering can be effectively used to characterize the structural details of "deep" nanostructures. In addition, it offers the additional advantage of measuring the buried interfaces, if needed. However, quantitative analysis of a typical x-ray diffraction pattern from a nanofabricated 2-D dot array (0.1- to 1-μm period) requires careful consideration of the resolution function of the probe [1], because its reciprocal space density is many orders of magnitude higher than those of typical solid-state or biological crystals. Consequently, the measured diffraction pattern exhibits characteristic features [1] as a result of the highly anisotropic nature of the instrumental resolution function.

Methods and Materials

For this study, a square array of circular disk-shaped dots with a period of 750 nm and a diameter of 340 nm was fabricated by using a standard lithography and liftoff process. The required pattern was written in a single polymethylmethacrylate (PMMA) layer with e-beam lithography, and a Gd film with a nominal thickness of 50 nm was deposited by using e-beam. An area of 0.5×0.5 mm^2 was patterned on a 10×10 mm^2 Si/SiO_2 wafer. X-ray diffraction measurements were performed by using 9 keV ($\lambda = 1.3776$ A) monochromatic x-rays at SRI-CAT beamlines 1-BM and 2-BM and beamline station 4-ID-D at the APS. The incident beam with its angular divergence of 1 mrad (horizontal) and 0.05 mrad (vertical) was used. The diffracted beam was collected by a scintillation detector with 1 mrad (horizontal) and 0.1 mrad (vertical) acceptance.

Results and Discussion

We define a coordinate system such that the *xz*-plane coincides with the vertical scattering plane and the *z*-axis is perpendicular to the sample surface. As depicted in the insets of Fig. 1, the azimuth angle ϕ measures the rotation of the reciprocal axes q_x and q_y with respect to the *x*-axis and *y*-axis about the *z*-axis.

Since the measurements presented here were made at a fixed q_z value of 0.18 A^{-1}, a point in the reciprocal space is indexed by using only two indices (H, K), by using the relationships $q_x = (2\pi/a)H$ and $q_y = (2\pi/a)K$, where a is the period of the nanoarray. Consequently, a radial [$q_r = \mathrm{sqrt}(q_x^2 + q_x^2)$] scan through a reciprocal point (H, K) was carried out by performing a theta rocking scan at $\phi = \tan^{-1}(K/H)$. Since the patterned area is much smaller than the total area of the substrate, the diffuse scattering from the substrate surface was subtracted by using the dynamical expression in Ref. 2 [see the dashed lines in Fig. 1(a) and (b)], and the diffraction intensities from the dot array were then obtained, as shown in Fig. 2.

The mathematical diffraction pattern constructed from a 2-D square dot array consists of 1-D rods along q_z direction, going through (H, K) integer points. Thus, a 2-D diffraction pattern at a fixed q_z value corresponds to a set of discrete intensities at (H, K) integer points. Experimentally, however, a typical q_r scan along the (H K) direction yields a number of peaks at noninteger positions, with the exception of that along the (1 0) direction. For example, a q_r scan along the (3 1) direction produces noninteger peaks at (3n/10, n/10), as shown in Fig. 2. In fact, these noninteger peaks are not points but are the cross sections of streaks.

We attribute the observed diffraction pattern to the resolution function, which describes the broadening of the reciprocal resolution of the probe as being primarily due to the divergence of the incident beam and the finite acceptance of the detector. The resolution function projected onto the q_x-q_y plane can be described as an ellipse with its minor and major axes parallel and perpendicular to the q_r direction. The lengths of the minor and major axes are $k_0 \Delta\psi$ and $k_0 \theta\Delta\theta$, respectively, where $\Delta\psi$ and $\Delta\theta$ are effective horizontal and vertical angular broadenings. The grazing incident geometry ($\theta << 1$) and our experimental setup with a smaller vertical divergence and a smaller detector acceptance make the elliptical sampling area virtually a stripe, with the ratio of length to width being a few hundred, as illustrated in Fig. 1(B). Consequently, the measurement performed at an arbitrary point, $\mathbf{G}_0 = (H, K)$, picks up the intensities from the neighboring diffraction rods $\mathbf{G} = (h, k)$ within the sampling area. A simple condition in which $\mathbf{G}_0$, $\mathbf{G}$, and $(\mathbf{G} - \mathbf{G}_0)$ form a right triangle can be expressed as $h H + k K = H^2 + K^2$.

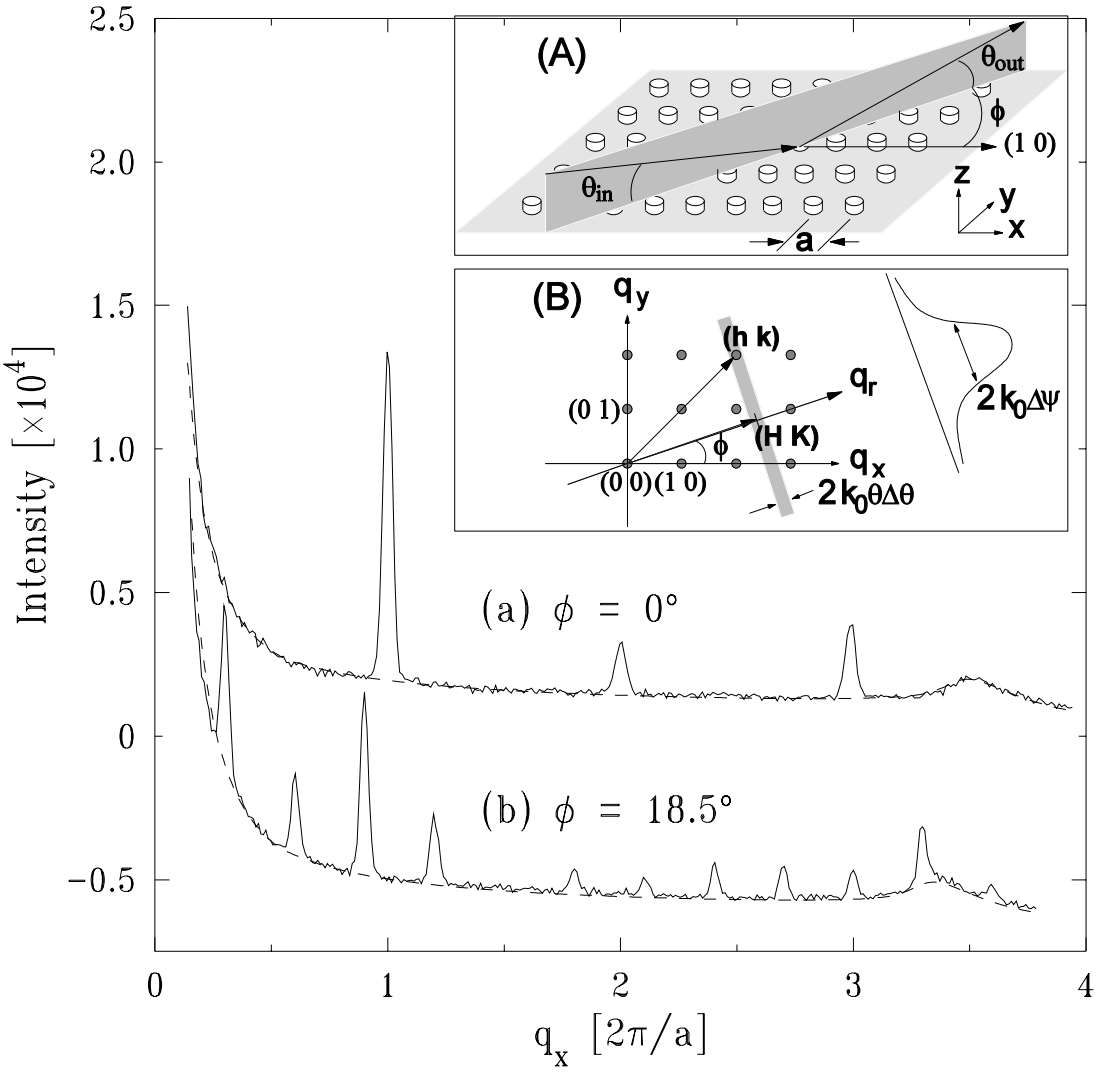

FIG. 1. Radial scans measured along (a) the (1 0) (ϕ = 0) direction and (b) the (3 1) (ϕ = 18.5) direction from a Gd dot array. Dashed lines represent the calculated diffuse scattering intensities from the substrate surface. Insets (A) and (B) show schematics of the scattering geometry and its corresponding diffraction configuration in the reciprocal plane. The gray stripe represents the resolution volumes when scanning along q_r.

As seen from the scanning electron microscopy (SEM) image in Fig. 2(d), dots are not a simple disk; instead, they have a thin "crown" on the top as a result of the photoresist removal process, as illustrated in Fig. 2(c). This finding was also confirmed by our atomic force microscopy (AFM) measurements, although the exact profile of the crown could not be measured. The solid line in Fig. 2 represents the diffracted intensities calculated for this crown model and shows good agreement with measurements. On the other hand, the dashed line calculated from a model of simple rings, as depicted in Fig. 2(b), overestimated the intensities at high q_r's. The details of this work are given in Ref. 3.

Acknowledgments

Use of the APS was supported by the U.S. Department of Energy (DOE), Office of Science, Office of Basic Energy Sciences, under Contract No. W-31-109-ENG-38.

References

[1] D. Rafaja, V. Valvoda, J. Kub, K. Temst, M.J. Van Bael, and Y. Bruynseraede, Phys. Rev. B **61**, 16144-16153 (2000).

[2] S.K. Sinha, E.B. Sirota, S. Garoff, and H.B. Stanley, Phys. Rev. B **38**, 2297-2311 (1988).

[3] D.R. Lee, Y.S. Chu, Y. Choi, J.C. Lang, G. Srajer, S.K. Sinha, V. Metlushko, and B. Ilic, Appl. Phys. Lett. **82**, 982-984 (2003).

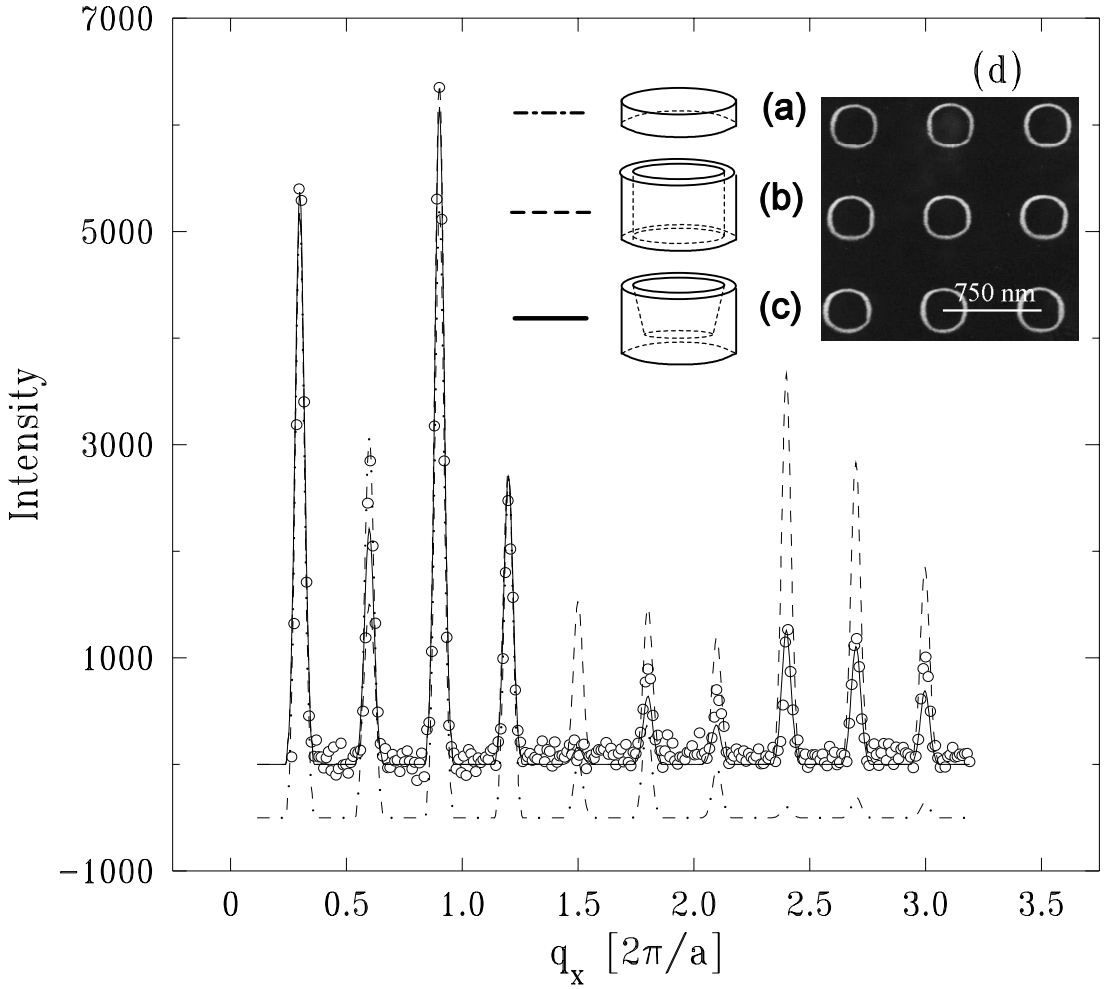

FIG. 2. Diffraction intensities of the radial scan along the (3 1) direction (ϕ = 18.5) after subtracting diffuse scattering intensities from the substrate surface. Circles represent measurements, and lines represent the calculations with different models: (a) circular disks (dashed-dotted line), (b) ring cylinders (dashed line), and (c) crowns (solid line). For clarity, the dashed-dotted line is shifted. Inset (d) shows a SEM picture from the sample.